# A NOVEL TECHNIQUE TO IMPROVE MEASUREMENTS IN TIME-OF-FLIGHT BASED ACOUSTIC TOMOGRAPHY

by © Justin Blackwood A Thesis submitted

to the School of Graduate Studies in partial fulfillment of the

requirements for the degree of

Master of Engineering

Memorial University of Newfoundland

May 2022

St. John's Newfoundland and Labrador

# Abstract

Understanding the changes in oceanographic conditions is important for many applications; from weather forecasting, studying the impacts of climate change and for safety considerations during operations at sea, such as offshore oil installations or offshore wind turbine sites. Many oceanographic parameters, such as temperature, current speed, salinity and pressure, can be derived using acoustic tomography techniques, which determine the time-of-flight between two points and then calculate the properties based on the bi-directional travel times.

Initial work in the field of time-of-flight acoustic tomography had focused on the mesoscale (100-1000s of kilometers). More recently, smaller scale systems have been tested that cover systems in the 100s of meters. This new range presents new challenges such as multipath propagation and the impact of timing errors on the scale of milliseconds. If these systems are to become successful, it will be essential to improve upon the precision and accuracy of the measurements obtained.

A new approach has been proposed and system developed to test its merits. This system utilizes an additional, third hydrophone to observe the waveform in the aqueous environment which is used in place of an ideal waveform in the data analysis. Where possible, to reduce sources of error, shore-side laboratory equipment was utilized for their robust prior testing and manufacturing quality and physical connections were utilized to prevent timing error.

# Acknowledgements

This project was made possible by the assistance of many people who I want to thank for their assistance:

Dr. Vlastimil Masek for offering to supervise my studies and guide me through the associated trials and tribulations

The staff at the Ocean Engineering Research Centre, especially Trevor Clarke, who assisted in conducting the experiment

My Fiancée, Annagray Campbell, for motivating my efforts and pushing me to continue with this research, especially as the difficulties and frictions endured due to covid-19, which impacted the pace of progress greatly

A big thank you for those listed as well as everyone who contributed to this work!

Table of Contents

*Abstract* ..... *ii*

Acknowledgements ..... iii

*List of figures* ..... *vi*

*List of figures (continued)* ..... *vii*

*List of Abbreviations* ..... *viii*

*Chapter 1: Introduction* ..... *1*

1.1 Literature Review ..... 2

1.2 Problem Statement ..... 6

1.3 Research Objectives ..... 7

1.4 Organization ..... 8

1.5 Conclusion ..... 8

*Chapter 2: Background* ..... *9*

2.1 Overview ..... 9

2.2 Comparison of Techniques ..... 10

2.3 Conclusion ..... 14

*CHAPTER 3: Experimental Setup* ..... *15*

3.1 Hypothesis ..... 15

3.2 Hardware ..... 15

3.3 Location ..... 16

3.4 Overview ..... 18

3.5 Positioning the hydrophones ..... 19

3.6 Reference Measurements ..... 21

3.7 Conclusion ..... 22

*Chapter 4: System Development* ..... *23*

4.1 System Design ..... 23

4.2 Testing ..... 26

4.3 Conclusion ..... 32

*CHAPTER 5: Data Analysis* ..... *33*

5.1 Analysis ..... 33

5.2 Resampling Data ..... 35

5.3 Results ..... 36

5.4 Conclusion ........................................................................................................38
*Chapter 6: Conclusion*........................................................................................*39*
6.1 Summary.............................................................................................................39
6.2 Future Work.........................................................................................................40
6.3 Conclusion ...........................................................................................................40
*Bibliography* .........................................................................................................*41*

# List of figures


| | | |
|---|---|---|
| Figure 1 | Topology of classic time-of-flight system | 11 |
| Figure 2 | Ideal signal as used in the old techniques analysis (x-axis is number of samples, not time) – Y-axis shown in volts | 12 |
| Figure 3 | Sample of initial pulses reaching the observer hydrophone, x-axis is time and y-axis is volts | 13 |
| Figure 4 | Signal measured at receiver, zoomed in on initial set of pulses received, x-axis is time and y-axis is in volts | 13 |
| Figure 5 | another example of the sub-sample of the observer hydrophone's data showing the first 10 pulses received, x-axis is samples and y-axis is time | 14 |
| Figure 6 | View looking down the towing tank towards to where the receiver was positioned | 17 |
| Figure 7 | Transmitter side of the towing tank showing the transmitting and observing hydrophone | 17 |
| Figure 8 | Layout of test props and equipment | 18 |
| Figure 9 | initial deployment of hydrophones at 1.0 m apart | 19 |
| Figure 10 | initial test trial showing the cross talk and received signal comingled | 20 |
| Figure 11 | crosstalk between transmitter and receiver circuits shown in isolation | 21 |
| Figure 12 | DeWalt laser measurement tool that was used for collecting measurement data between various segments of the system | 22 |
| Figure 13 | Arduino Uno Atmega168 schematic, zoomed in on a subset of pins | 24 |
| Figure 14 | Schematic of Class-D Amplifier | 25 |
| Figure 15 | Inverter to drive transmitting hydrophone (right) and its controller (Arduino Uno R3, left) | 26 |
| Figure 16 | gate signal distortion when system was connected to hydrophone, before adding shunt load resistor | 27 |
| Figure 17 | Gate signals after adding shunt resistor to output | 27 |
| Figure 18 | two hydrophones, placed in a small glass fish tank for initial testing | 28 |
| Figure 19 | Waveform received while hydrophones were physically touching in tank (left) versus a small separation (right) | 29 |
| Figure 20 | pre-amp circuits with tuneable gain via feedback potentiometer | |
| Figure 21 | Schematic of pre-amplifier receiver circuit | 30 |
| Figure 22 | Testing the pre-amp with a function generator input | 30 |

# List of figures (continued)


| | | |
|---|---|---|
| Figure 23 | pre-amp performance in the tow bank. Yellow is input signal and blue is output signal. | 31 |
| Figure 24 | The hydrophone signal recorded at the observing hydrophone (blue) and the receiver-side hydrophone (orange) | 32 |
| Figure 25 | table showing standard deviation versus cross-correlation inputs | 34 |
| Figure 26 | the original dataset (blue) which has been vertically offset above the resampled, version (orange) | 35 |
| Figure 27 | cross-correlation output from new technique (x-axis is in samples) | 37 |
| Figure 28 | cross-correlation output from the old technique (x-axis is in samples) | 37 |
| Figure 29 | cross-correlation results for all trials using a 200-sample window for the input signal (orange) and the original method approach shown in blue | 38 |

# List of Abbreviations

| | |
|---|---|
| ADCP | Acoustic-Doppler Current Profiler |
| EM | Electromagnetic |
| GNU | GNU’s not Unix (type of free software) |
| GPS | Global Positioning System |
| LDCP | Laser-Doppler Current Profiler |
| MODBUS | Serial communications protocol developed by Modicon |
| NMOS | N-type Metal-Oxide Semiconductor |
| OAT | Oceanographic Acoustic Tomography |
| OERC | Ocean Engineering Research Centre |
| PMOS | P-type Metal-Oxide Semiconductor |
| PWM | Pulse-Width Modulation |

# Chapter 1: Introduction

Understanding oceanographic conditions has been studied since early navigators took to the sea to explore. Understanding the trends of the ocean's currents was paramount to their safety and expeditious travel in these times. In more a modern context, oceanography has been important in the study of meteorology, climate change as well as for monitoring safe operating conditions for offshore installations such as wind turbines and oil platforms.

Throughout the latter half of the 1900s, many methods have been devised for studying ocean currents: monitoring free-floating objects, mechanical instrumentation, radar, acoustic and laser-based doppler sensors, to name a few. With the improvement in high-frequency electronics, as well as the advent of GPS technology, a new approach that utilizes short-range acoustic tomography (over 10s or 100s of meters) to determine the speed of ocean currents by measuring the speed of bi-directional transmission of sound across a channel of water. Thus far, these systems have experienced accuracy limitations, especially in acoustically noisy or shallow regions due to the inference from multipath effects as well from idealistic assumptions of the impact the channel has on the piezo-electric signal generated by the hydrophone.

The work detailed in this thesis introduces a novel approach to improve short-range acoustic tomography using an additional nearby hydrophone to provide feedback to aid in cross-correlation analysis. The custom-developed system employs hydrophones driven by a 12.5 kHz signal, a micro-controller system for transmitting and receiving data as well as oscilloscopes for capturing the signals received. This data was then cross-corelated to determine the distance between the transmitting and receiving hydrophones. There were two techniques compared in this analysis, one using ideal-waveform assumptions as a benchmark and the other using the 'listener' hydrophones in-situ data as the input signal. The new technique was shown to be both more accurate and less error-prone than the original technique.

## 1.1 Literature Review

There has been much research and field work performed over the latter half of the 20$^{th}$ century to quantify and understand oceanographic currents [2] [3]. Understanding oceanographic currents and temperature gradients can help further the fields of weather forecasting and climate change analysis, improve safety of offshore operations for oil installations and wind turbine sites as well as assist studies of marine wildlife [4] [5] [6]. Understanding the ocean's currents are also paramount for seafaring vessels, to this end, in addition to consulting maps of ocean currents, many vessels have current meters (ADCP) mounted to their hull to get real-time, location specific data on the state of the sea [7].

Many techniques have been developed for determining ocean current speed, direction and temperature gradients over the years. Some examples of oceanographic instrumentation techniques include mechanical current meters, acoustic-doppler and laser-doppler current profilers (ADCP and LDCP) and time-of-flight acoustic-based systems, just to name a few [5] [8]. Initially, instrumentation was primarily mechanical but, as electronics became more advanced, ultra-sonic current meters were developed that offered superior bandwidth and sensitivity than their mechanical counterparts [9].

Each of these techniques have pros and cons that make them well suited for specific applications. Different types of sensors are better suited for certain situations, depending on: spatial scale of measurements required, expected harshness of conditions (durability), length of deployment, etc. [8] [5] Mechanical current meters offer a single-point measurement. They can also be deployed in an array-configuration to give data over a larger region; however, this becomes impractical as the need for resolution increases. Similarly, the most basic technique for measuring temperature in a water column is a thermometer, which can be extended using a string of thermometers (i.e. thermistor array). With similar practical limitations for deployments requiring high-resolution over larger areas.

Expanding on the initial, basic measurement techniques, later research focused on the development of ADCPs that offer single-point measurement of ocean currents but are able to measure currents at various depths or 'bins' throughout the water column. ADCPs operate by transmitting a signal from one transducer at a fixed angle and then receive the backscatter for analysis. ADCPs depend on debris to be present in the water to provide the required backscatter [5]. This limitation makes ADCPs inadequate for certain bodies of water and even certain seasonal variations that do not have sufficient particles present to provide reliable backscatter. One anecdotal example of this effect is a reduction in the ability to measure near-surface currents from an upward-facing ADCP as the surface water warms and causes plankton and other sea matter to migrate to deeper depths, resulting in now data available for the upper portion of the water column. Depending on frequency of operation, ADCPs have a trade-off between range of measurement and minimum bin size, similar to the frequency-based range to bandwidth trade-off existing in other systems. A small set of ADCPs can be deployed in a water column of 100s of meters in depth and give measurements for bins in the low-single digits of meters. A deployment of ADCPs, as described, can be more efficient than deploying the equivalent system of hundreds of physical current meters.

Simultaneous field-study comparisons of different types of sensors have led to a better understanding of the ideal sensor type for different environments by being able to compare the instrument's readings based on the environment and timeline. One such finding was that while instruments mounted to a subsurface mooring are more stable than equipment mounted to surface buoys, measuring near-surface currents with subsurface sensors can be difficult. Conversely, ADCPs mounted to a surface float encounter issues when conditions result in the buoy being angled greater than 20 degrees, due to limitations in onboard compass units [8].

There is emerging research on using remote sensing methods either through shore-based sonar or satellite radiometry to measure ocean currents. Both approaches offer the benefit of not needing to deploy equipment in harsh ocean environments and are very scalable compared to previously developed systems. However, these electro-magnetic signal-based systems have the limitation of not being able to penetrate the ocean surface boundary to measure sub-surface currents.

In 2020, Tim Smith developed a system to measure tidal currents in a bay on the coast of Newfoundland [10]. This system measured the average current speed over a 130m gap at the mouth of a basin that experienced significant tidal current flow near the town of Bellevue. This system had two hydrophones deployed, both of which were cabled back to shore. It utilized a class-D amplifier, MODBUS-based time synchronization system and remote data collection via an Arduino Uno microcontroller. This system was powered by a 12V power source, located on shore and used a common cable to transmit data and power to each of the hydrophone's nodes and their respective circuitry (inverter, driver and microcontroller). The nodes alternated their operation as transmitter or receiver and would adjust their data acquisition accordingly by utilizing variable gain. The system compared bi-directional acoustic travel times to estimate the average current speed between the hydrophones. The data received at each hydrophone was compared against an ideal square-wave waveform that was used as the hydrophone's driving signal.

In the conclusion section of Mr. Smith's thesis, there were many lessons learned that could be applied to this thesis' work. Based on these lessons, where possible, sources of error or uncertainty were removed by simplifying the design such removing the data-over-power superimposed signals, utilizing high-quality lab-grade equipment whenever possible and using a physical co-axial connection to perform time-synchronization as opposed to a complex serial communications protocol implementation.

This thesis' objective is to improve upon part of the OAT system designed by Mr. Smith by attempting a novel technique that captures real-world signal data, between the transmitter and receiver and utilizes this data in the cross-correlation analysis. It is expected that this change will greatly improve upon the accuracy and precision of the results when compared to the original system.

Unrelated to Mr. Smith's work, an area of difficulty in measuring shallow water current speeds, using acoustic tomography, was found during the literature review for this work: interference caused by multipath effects. Currently, to counteract the arrival of certain multipath components that pre-date the initial, primary signal there is often an amplitude threshold applied to the signal analysis. This approach discounts smaller amplitude signals and instead assign a cut-off amplitude after which the detection of the intended arrival can be conducted. It is expected that this proof-of-concept will improve the accuracy of OAT without utilizing the threshold approach and instead focusing on accurately representing the initial signal used in data analysis.

## 1.2 Problem Statement

Due to multi-path effects, it can be difficult to assess a received acoustic signal and isolate the intended signal from similar artifacts generated through interaction with the water column environment [11]. In Tim Smith's experiments [10], he utilized a time-of-flight analysis technique which employed cross-correlation calculations on a received waveform against a hydrophone input signal waveform. Mr. Smith's system also based time-of-flight analysis on microcontroller measured timing as opposed to measuring the signal after electro-piezo excitation of the hydrophone.

Upon reflection on how to improve upon these initial experiments, this thesis will implement a similar experiment, in a more controlled environment, using a measured waveform after the electro-piezo coupling of the hydrophone (utilizing an additional hydrophone). There are also characteristics of the acoustic system that impact the acoustic signal between transmission and reception [11]. These variances from an ideal impulse are due to the transfer functions of the transmission medium, as well as transmitter and receiver piezo-electric characteristics. The hypothesis is that using this measured signal, in the water column, will make the cross-correlation analysis more accurate as well as more precise.

Furthermore, in Tim's thesis [7] there is a requirement to correct for timing due to it being timed at the microprocessor (hydrophone driver circuit) as opposed to referenced to the acoustic signal in the water, which is expected to remove a source of uncertainty and error.

## 1.3 Research Objectives

This thesis details the design, testing and analysis of an acoustic time-of-flight system that seeks to improve the accuracy and precision of cross-correlations of acoustic signals in an acoustically noisy environment due to many sources of multi-path interference that increase the likelihood of successful, accurate time-of-flight data acquisition.

This thesis was inspired in part by the findings of Tim Smith's 2020 thesis titled 'Measuring Marine Currents Using Underwater Acoustics' [10]. Many of the design decisions for the experiments detailed in this document were made to remove many of the sources of error and uncertainty in Mr. Smith's thesis. Based on Tim's experiences, it was determined that in order to isolate the merit of the proposed technique, sources of error such as time synchronization, accuracy of custom-built data acquisition equipment as well as practical issues arising in the field such as the need to estimate physical distances in the ocean (as opposed to being able to obtain highly accurate range data).

## 1.4 Organization

The thesis is arranged in the following sections:

Chapter 1: Introduction

Chapter 2: Background

Chapter 3: Experiment Setup

Chapter 4: System Development and testing

Chapter 5: Data Analysis

Chapter 6: Conclusion and Future Work

## 1.5 Conclusion

Understanding the ocean's currents has been an important field of study for hundreds of years and remains so today. This field aids in transportation and meteorology industries, as well as safety and risk reduction efforts for various installations. This thesis introduces a novel approach to improve upon the previous work of Mr. Smith [10]. By adding an additional hydrophone to measure the in-situ signal and use this as feedback for signal analysis to determine time-of-flight. This data could be used to determine many oceanographic conditions such as velocity of currents, salinity and temperature.

# Chapter 2: Background

## 2.1 Overview

Oceanographic measurements can be obtained using a variety of technologies: mechanical systems, semiconductor-based sensors, satellite imagery, radar back scatter, doppler-effect sensors and acoustic propagation are just some of these techniques [8, 12]. Each approach has its own pros and cons which make them ideal for different applications.

When the objective is to measure ocean currents, ADCPs and Acoustic Tomography are the two prevalent techniques. Historically, tomography was utilized for large-scale measurements on the mesoscale (10s or 100s of kilometers) while ADCPs are used to measure more locally, at a single point in the water column. More recently, utilizing higher-frequency hydrophones, tomography has been modified to measure current speeds over smaller regions on the order of 10s or 100s of meters.

The speed of sounds is a function of temperature, salinity and pressure [13] [5]. The most significant factor varies depending on position in the water column. Near the surface, temperature is the most prevalent factor while at deeper portions, temperature becomes more constant and such that pressure becomes the most dominant of the factors. The speed of sound increases with both increasing temperature and increasing pressure, creating an asymmetric, horizontal-parabolic curve for a typical oceanographic environment with speeds initially decreasing through the upper water column then pivoting to decrease once the water temperature starts to stabilize.

The ocean acts as a good carrier for sound, especially compared against its transmission properties for Electro-Magnetic radiation [13]. For this reason, the piezo-electric coupling offered by a hydrophone offers a great tool for instrumentation to measure oceanographic parameters beneath the surface. Acoustic travel times can be used as the basis for acoustic tomography and thermography measurements [14]. Previous works have shown that frequencies in the audio range can be used to conduct distance measurements in aqueous environments [13] [14].

Furthermore, since as frequency increases, signals attenuate greatly in an aqueous environment, there is little benefit from choosing a higher frequency aside from electronics design perspective or perhaps, for data transmission systems in which the higher frequency offers an increased bandwidth trade-off versus distance for transmission.

## 2.2 Comparison of Techniques

The "old technique" (using two hydrophones) involved computing the cross-correlation of an ideal waveform, in this case a train of ten pulses, representing the signal used to excite the transmitting hydrophone against a received signal. The ideal waveform, by its theoretical nature, is uniform and does not have distinguishing characteristics as would exist in a measured signal. However, in a two-hydrophone signal, it would not be possible to use a measured signal in the data analysis.

Below in figure 1, a unidirectional section of a time-of-flight tomography system is detailed. The transmitting hydrophone is excited by an inverter which outputs a high voltage sinusoid which then creates a piezo signal that permeates through the water until it is observed at the receiving hydrophone, some distance away. This process is then performed in reverse and by using the resultant data analysis can be used to determine the properties of the water between the hydrophones, on average during the time of transmission.

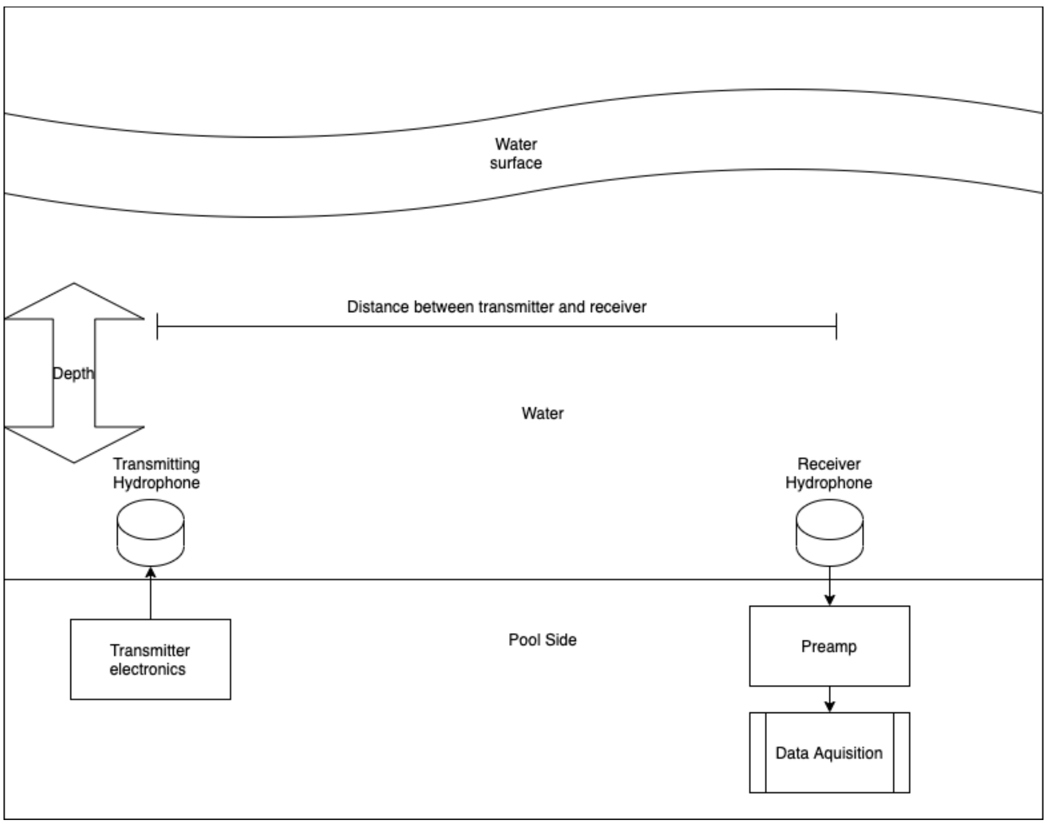

Figure 1: topology of classic time-of-flight system

While this system has proven a useful technique for determining properties in a water column, there is room to improve upon the accuracy and precision of the time-of-flight system which are subject to inaccuracies caused by reflections, multi-path receptions, high signal-to-noise, etc [14]

.

The hypothesis of the experiment that this thesis is based upon was that by improving the input signal used in cross-correlation analysis, that the system's performance will improve. By observing the piezo signal in the aqueous environment, with the impact of the channel having already started, the imperfections of the signal captured are used to identify the uniqueness of the transmitted signal in the received signal which has elements of the transmitted signal mixed with various multipath artifacts as well as constructive and destructive interference. It is also expected that timing the system based on the acoustic signal measured as opposed to its electric-excitation (at the micro-controller driver-circuit level), that this will remove a source of uncertainty and improve accuracy by capturing the acoustic signal; after it has been produced by the hydrophone, and consequently improve the system's accuracy. Below in Figure 2, the ideal transmitted signal used in the old technique is shown.

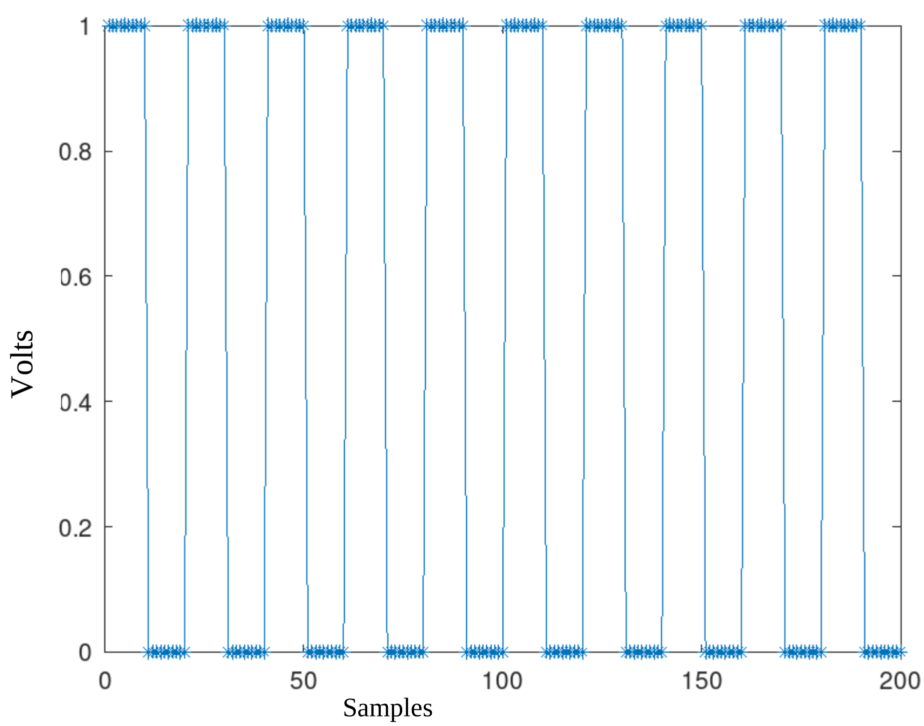


Figure 2: ideal signal as used in the old techniques analysis (x-axis is number of samples, not time) – Y-axis shown in non-specified units, representative of volts

Figures 3 and 4 below show experimental data for the transmitted and received signals, respectively. Finally, Figure 5 shows an additional experimentally measured signal measured by the observer hydrophone, proximal to the transmitter.

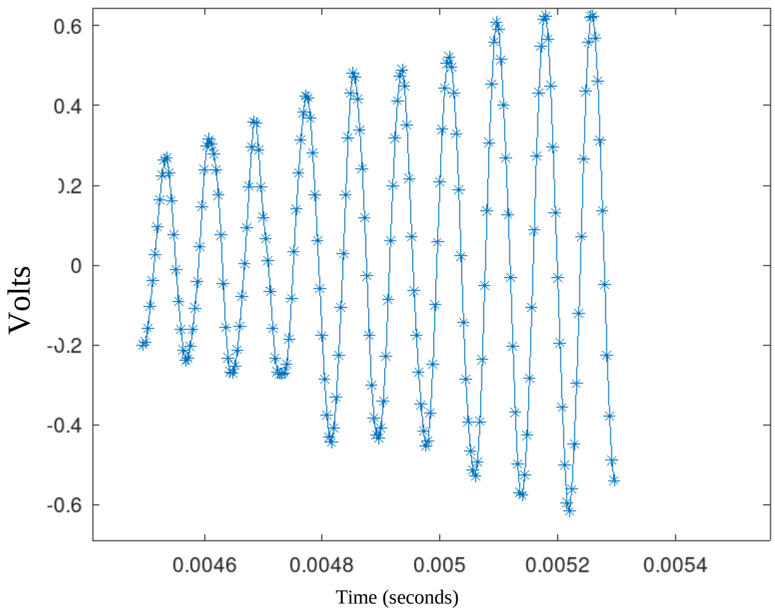


Figure 3: sample of initial pulses reaching the observer hydrophone, x-axis is time and y-axis is volts

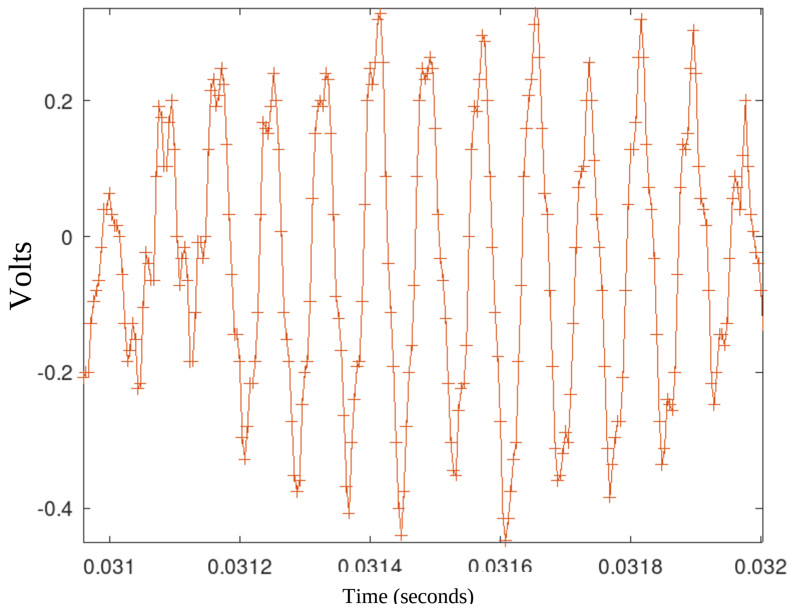


Figure 4: signal measured at receiver, zoomed in on initial set of pulses received, x-axis is time and y-axis is volts

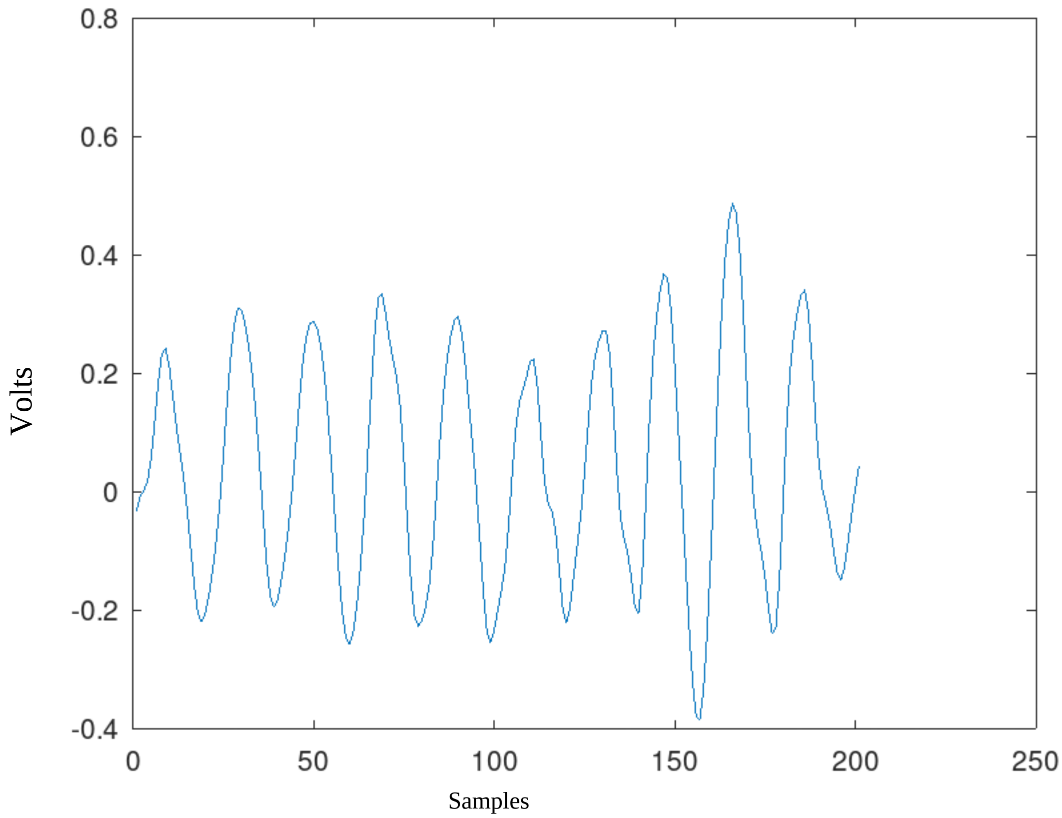


Figure 5: another example of the sub-sample of the observer hydrophone's data showing the first 10 pulses received, x-axis is samples and y-axis is volts

## 2.3 Conclusion

In conclusion, this section describes the difference in techniques between Mr. Smith's experiment and the work of this thesis. The signal observed by the additional hydrophone captures the irregularity of the signal in the channel compared with the ideal signal used to excite the hydrophone. These differences have an impact on the signal analysis performed which led to improved outcomes form the signal analysis of the observed time-of-flight.

# CHAPTER 3: Experimental Setup

## 3.1 Hypothesis

The experiment performed as part of this thesis aimed to assess a new technique for improving the accuracy of cross-correlation analysis for time-of-flight acoustic tomography. The hypothesis was that measuring the signal just after transmission and using that waveform, in place of a hypothetical and ideal waveform, would improve the accuracy of the cross-correlation results. In order to measure the signal near the transmission source, an additional third hydrophone was added to the system in addition to a second oscilloscope to make the local measurements.

## 3.2 Hardware

The hardware for this experiment were custom-made and were tested individually before being integrated into the overall system. The overall system consisted of a class-D inverter and two pre-amplifiers, one for each of the listening hydrophone.

The inverter was designed to work at 12.5 kHz. The gate driver and control action were performed using an Arduino uno microcontroller. A push button was connected to the Arduino which allowed for each triggering of the driving signal while the number of pulses was configured using the interrupt pin aired with logic in the microcontroller's programming that would stop the PWM output after 10 pulses and re-initiate the PWM once the button was pressed again.

Initially, the inverter did not generate a clean waveform. From previous experience, it was determined that this was most likely due to an overly capacitive loading and a shunt 1 k resistor was added to the output of the inverter, which then significantly improved the output measured at the load.

## 3.3 Location

The experiment was conducted at the Ocean Engineering research Centre (OERC) Towing Tank on the first floor of the S.J. Carew building on Memorial University's campus in St. John's. The tank is 54.7 meters long and has a maximum depth of 3.04m. The tank was designed to support experiments in the fields of ship building and offshore research. The experimental environment is show below in Figures 6 and 7. Figure 6 (below) shows a view of the Towing Tank with the mobile platform in the background while Figure 7 shows the transmitting hydrophone (background) and the observing hydrophone (foreground).

Figure 6: View looking down the towing tank towards to where the receiver was positioned


Figure 7: Transmitter side of the towing tank showing the transmitting and observing hydrophone

## 3.4 Overview

The set up for the experiment involved three hydrophones, an inverter, two preamps and two oscilloscopes, oriented as shown in Figure 8, below. The transmitting hydrophone and observer hydrophone are 10.01m apart while the transmitter and receiver are separated by 45.8m. The inverter is connected to the transmitting hydrophone and is controlled by an Arduino that generates ten pulses, at 12.5 kHz, when an attached push-button is pressed. This button press starts a chain of events that excites the transmitting hydrophone and initiates the capture of data acquisition from the observer and receiving hydrophones.

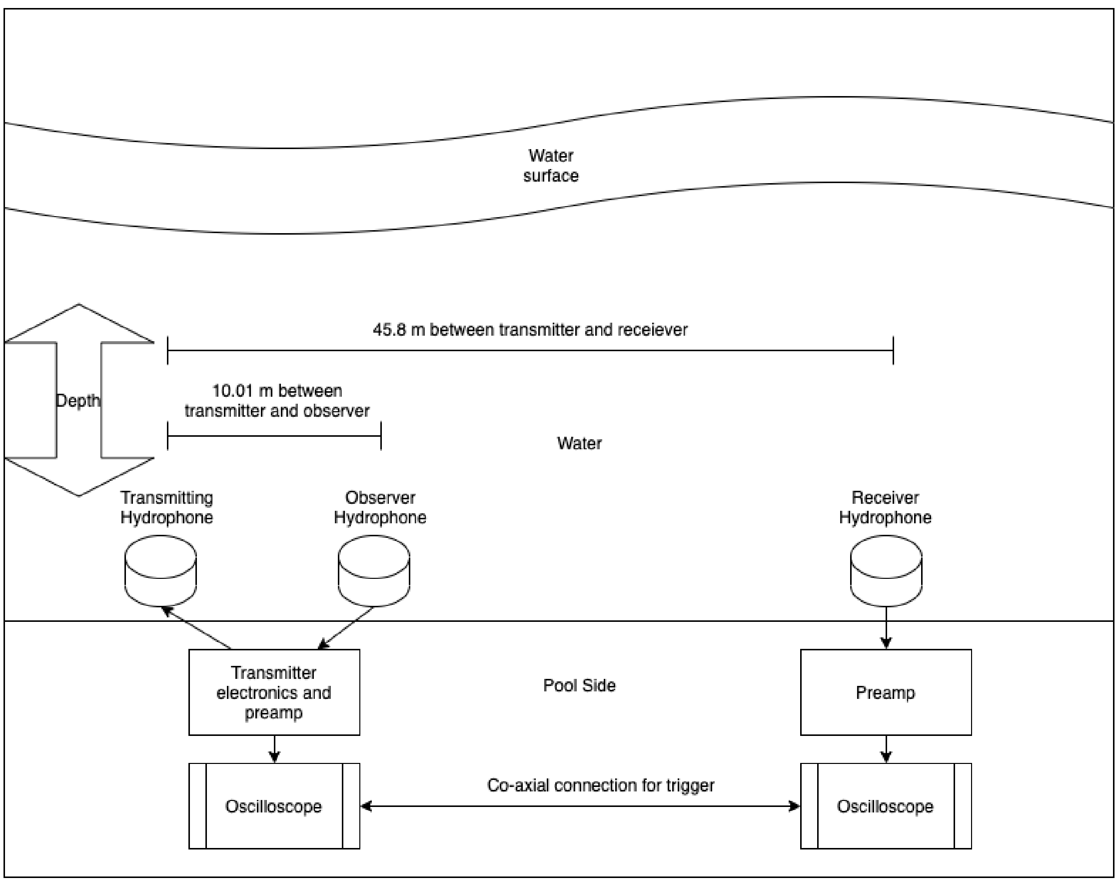

Figure 8: Layout of test props and equipment

## 3.5 Positioning the hydrophones

When deciding where to place the observing hydrophone with respect to the transmitter, the initial assumption was that any distance that placed the observer outside of near field of the transmitter. The near field [15] can be defined in a few ways, the easiest to visualize is D >> wavelength. Given the aqueous environment and assuming a speed of sound in water of 1500 m/s and an operating frequency of 12.5 kHz, it can be calculated that the wavelength is 0.12m and therefore, the initial distance of 1.0m was chosen. Conveniently, the platforms bringing across the towing tank were 1.0 m wide, and the hydrophones were initially deployed on either side of the platform, as shown below in Figure 9.

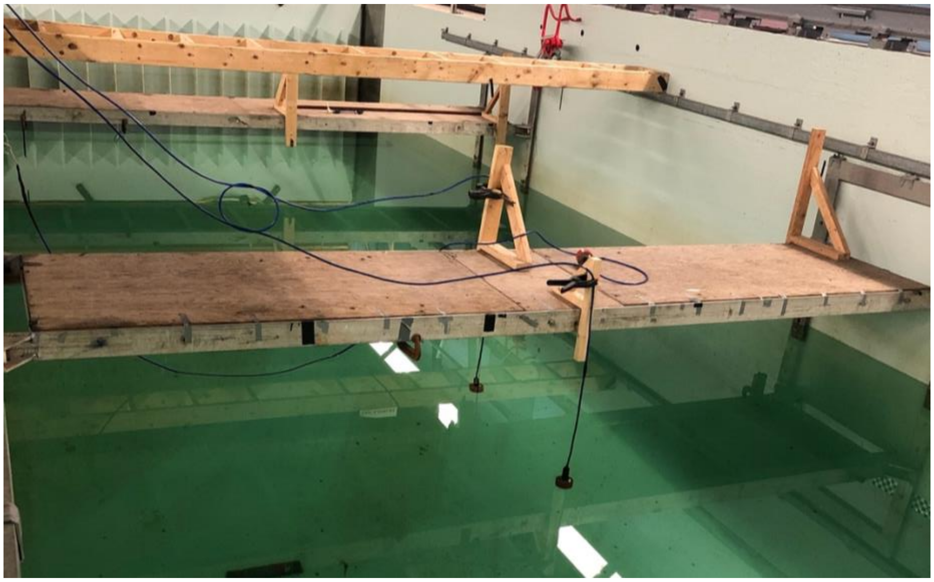

Figure 9: initial deployment of hydrophones at 1.0 m apart

The result of this first experiment was that the received signal appeared to be comingled with a crosstalk signal coming from the transmitter's signal; this can be seen in Figure 10, below. Removing the observer from the test pool, the crosstalk was still present and now clearly distinguishable from the received signal present in the previous trial; this can be seen in Figure

11. The crosstalk is most likely present due to the stepped-up voltage applied to the hydrophone, creating large EM fields near the op-amp. At this point, rather than attempt to shield the transmitter and receiver circuitry, it was decided that moving the observer hydrophone to a greater distance would be the more practical fix for this issue. The crosstalk is present in all the future trials of the experiment, however, with the hydrophone positioned at 10.01 m instead of 1.0m, the observed waveform was safely separated in time from the crosstalk.

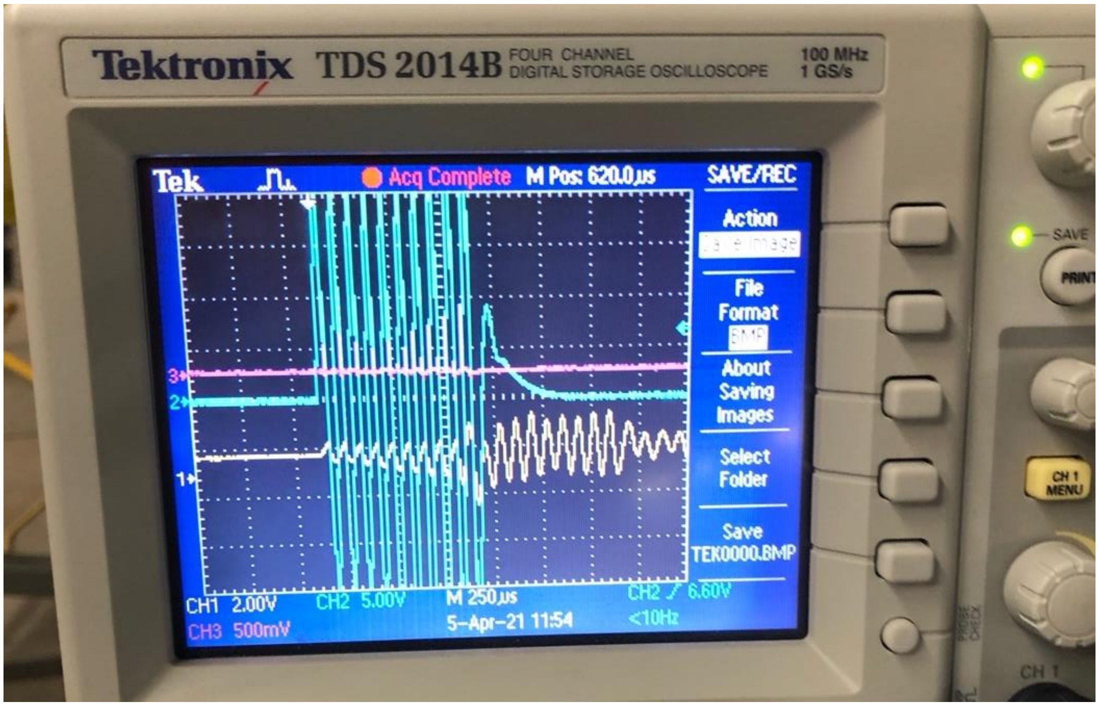

Figure 10: initial test trial showing the cross talk and received signal comingled

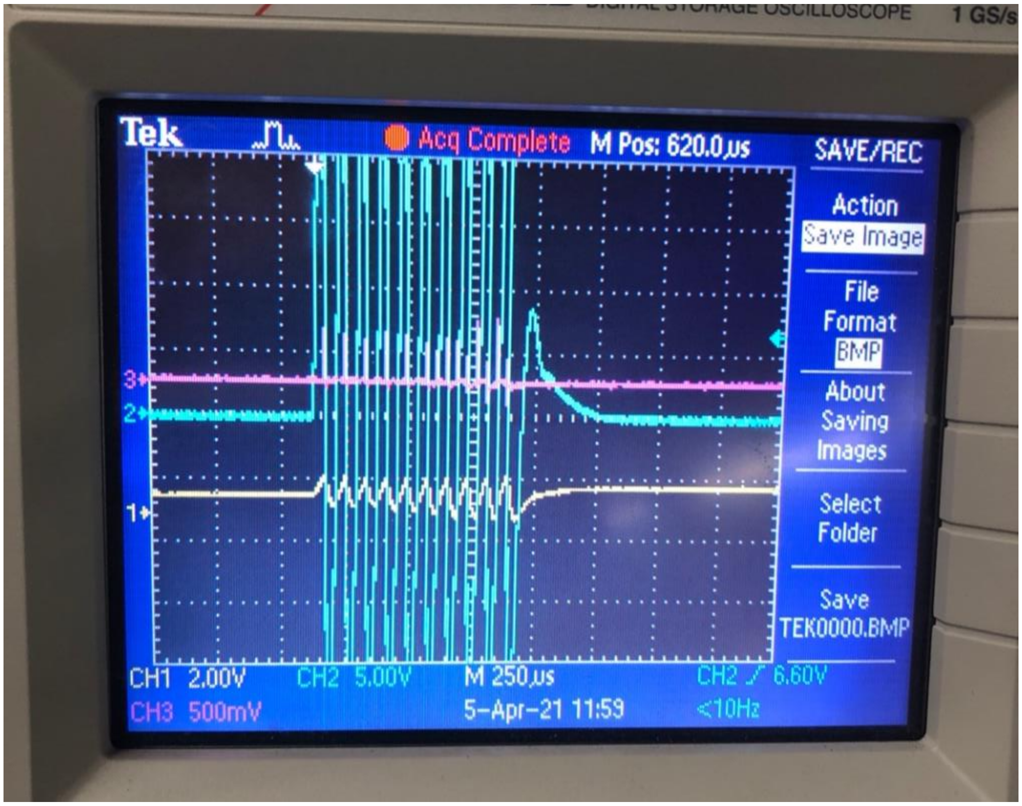

Figure 11: crosstalk between transmitter and receiver circuits shown in isolation

## 3.6 Reference Measurements

Two types of measurements were required to perform the data analysis from this experiment: acoustic data measured from the receiving hydrophones and the physical distances between the hydrophones. The distance between the hydrophones was determined using a laser-based distance meter made by DeWalt which are shown in Figure 12, below.

The voltage signal from the hydrophones was obtained via oscilloscope. The oscilloscopes were Tektronix TDS 2000 series oscilloscopes. The data was captured using single-shot mode and was recorded to a USB stick after each trial was completed. The data was then brought together from the two scopes and amalgamated for analysis. Both oscilloscopes were triggered by the first rising edge of the inverter's driving signal. The scopes were connected physically by coaxial cable to achieve optimal time-synchronization.

Figure 12: DeWalt laser measurement tool that was used for collecting measurement data between various segments of the system

## 3.7 Conclusion

In summary, this section details the location and test setup for the experiment that forms the foundation of this thesis. A series of pre-experiment in-situ testing led to some adjustments to the original plan and ensured results that were suitable for further analysis. By adjusting physical distances to mitigate crosstalk overlapping with the recorded signal, there was no longer and concern on the distortion this may have applied to the observed signal.

# Chapter 4: System Development

## 4.1 System Design

The first portion of the system developed was the controller for the transmitting hydrophone and its inverter. The Arduino Uno was chosen for this task due to its affordable price, ease of programming (including importable libraries) and all the required pins were broken out for easy prototyping.

The Arduino has two external interrupt pins (pin 2 and 3); these were used to provide easy control of the hydrophone driver by allowing for one interrupt to be a ‘start button’ to be established using a push-button switch connected to ground and the other interrupt implemented a counter for the number of pulses outputted from the PWM pin which allowed for a software-configured pulse count to be implemented.

By default, the Arduino PWM signal is relatively slow at 488 or 976 Hz (depending on the pin). Thankfully, by adjusting internal registers, the frequency can be boosted to up to 1 MHz.
This is made easier again by an open-sourced library, ‘FastPwmPin’ which makes increasing the frequency as easy as using a function call.

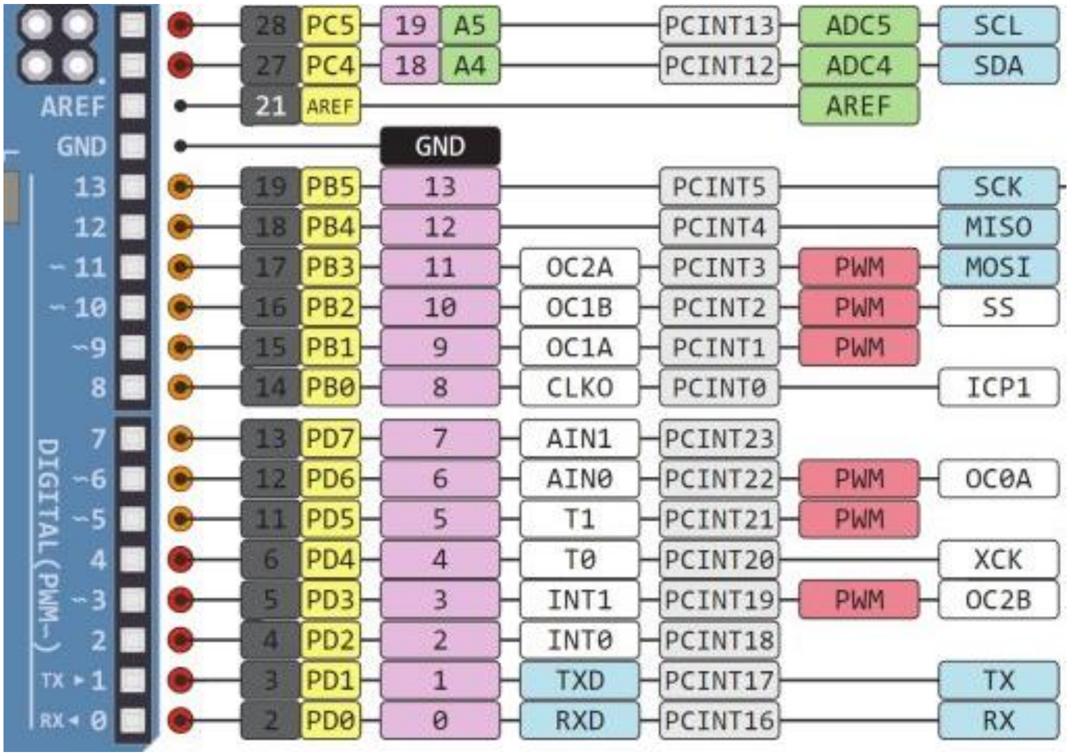


Figure 13: Arduino Uno Atmega168 schematic, zoomed in on a subset of pins
Source: https://forum.arduino.cc/t/arduino-uno-cnc-shield-software-pwm/674570

The inverter was designed to be the same as the one used in Tim Smith's thesis. This design uses a class-D amplifier topology, implemented using one NMOS and one PMOS transistor that utilize the same driving signal. In order to ensure break-before-make operation, inline capacitors were applied to one of the gates to offset the waveforms and prevent a shoot-through condition. Unlike a typical class-D amplifier, this inverter switches on the low side of a transformer and provides a boosted voltage output signal for the hydrophones. See Figure 14 and Figure 15 below for visual representations of this circuit. The PWM driver signal was also used as feedback into an interrupt pin on the Arduino to ensure a fixed number of ten pulses was sent with each run of the system. The interface between the Arduino and the inverter can be seen in Figure 15 below, on the left-hand side there are 3 wires (2 blue and one brown), the brown wire is the PWM driving signal while the upper blue wire is connected to the push-button that restarts the system and the lower blue wire is the feedback to the interrupt that stops the system after generating ten pulses. Figure 13 above shows the schematic of the pins in this region of the Arduino, for reference.

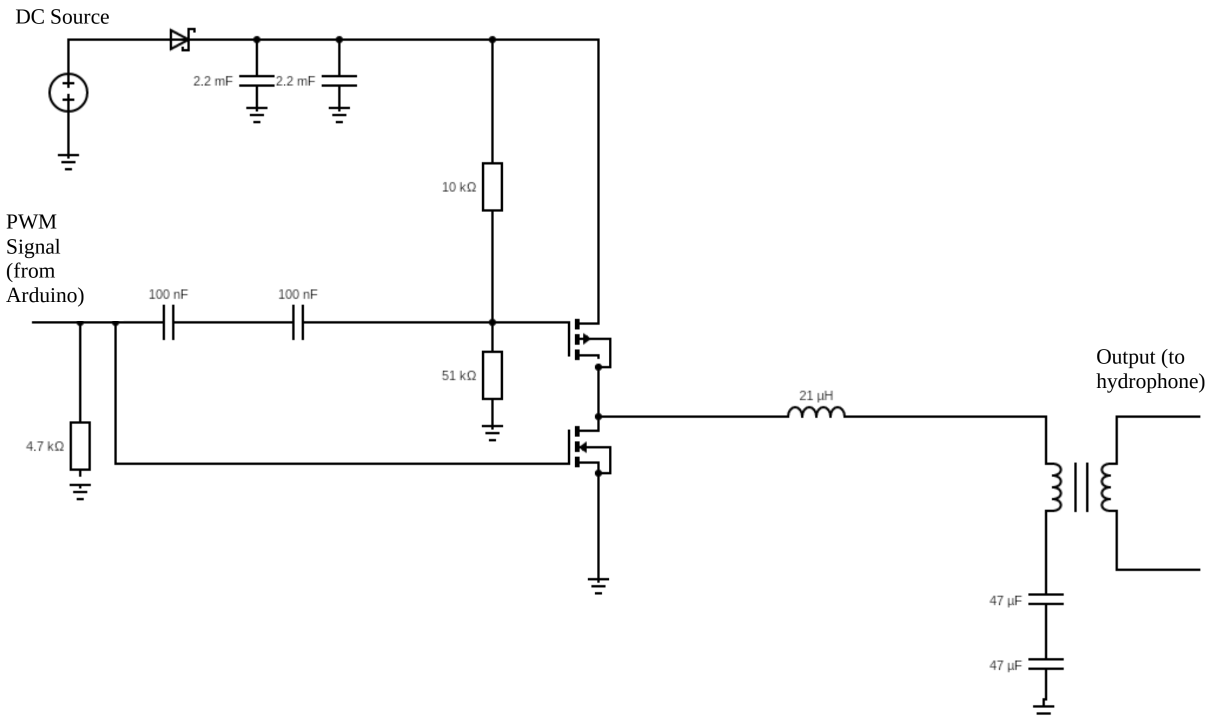


Figure 14: Schematic of class-D inverter

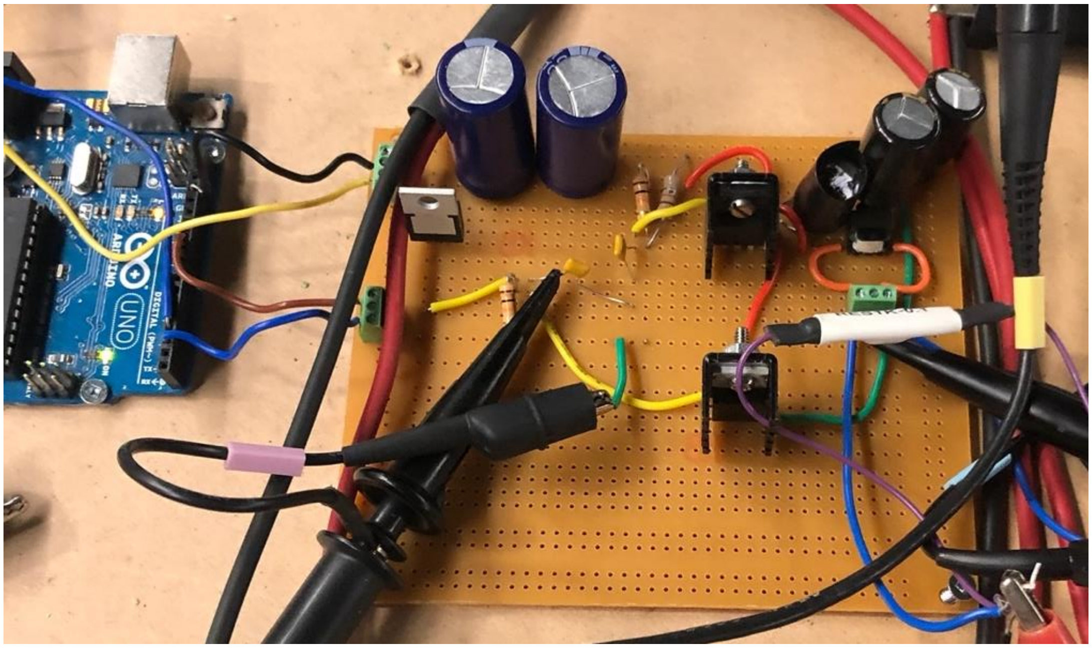
Figure 15: Inverter to drive transmitting hydrophone (right) and its controller (Arduino Uno R3, left)

## 4.2 Testing

While testing the interfacing of the Arduino controller with the inverter and its hydrophone load, it was noticed that the output voltage was irregular and non-sinusoidal. Drawing on previous experiences in inverter design, I knew that excessively capacitive loading can be a source of distorted output waveforms and tested connecting a parallel-shunt resistor to reduce the distortion. This change quickly resolved the issue and for the remainder of the development and subsequent experiment, a 1 kΩ resistor was in parallel with the output of the inverter.

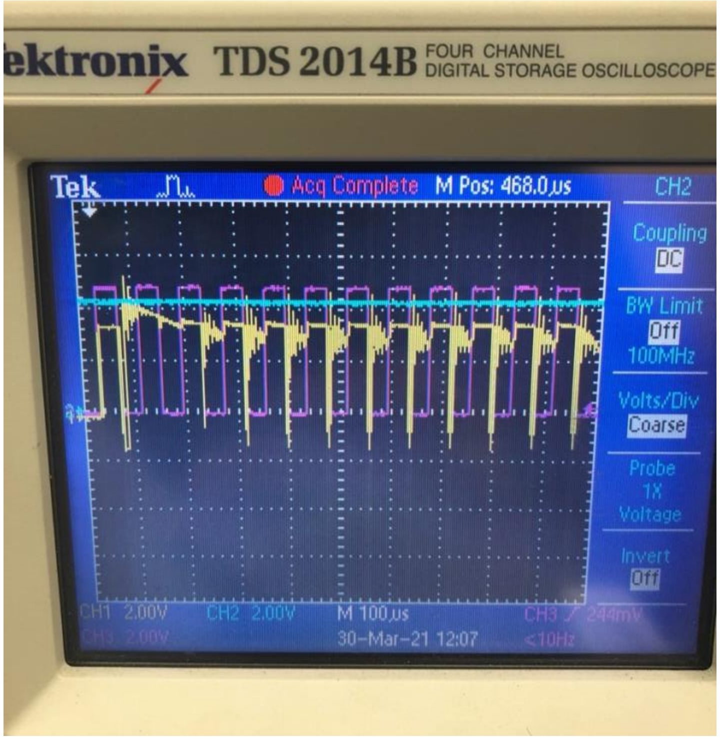


Figure 16: gate signal distortion when system was connected to hydrophone, before adding shunt load resistor

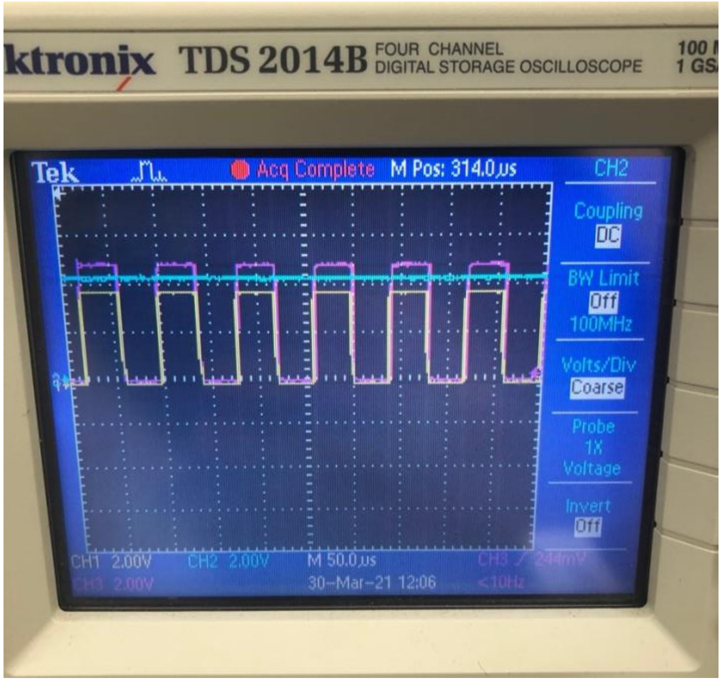


Figure 17: Gate signals after adding shunt resistor to output

Once the waveforms looked good on the transmitting side, it was time to test the receiving side of the system. In a fish tank, the hydrophones were laid initially touching and then slightly apart, so test reception as well as signal attenuation. Even at this relatively small displacement, the attenuation of the acoustic signal in water was very apparent. At this point, it became obvious that even for the observing hydrophone, a pre-amp would be required for data acquisition; the approximately 30 cm of separation had greatly reduced the quality and amplitude of the received signal.

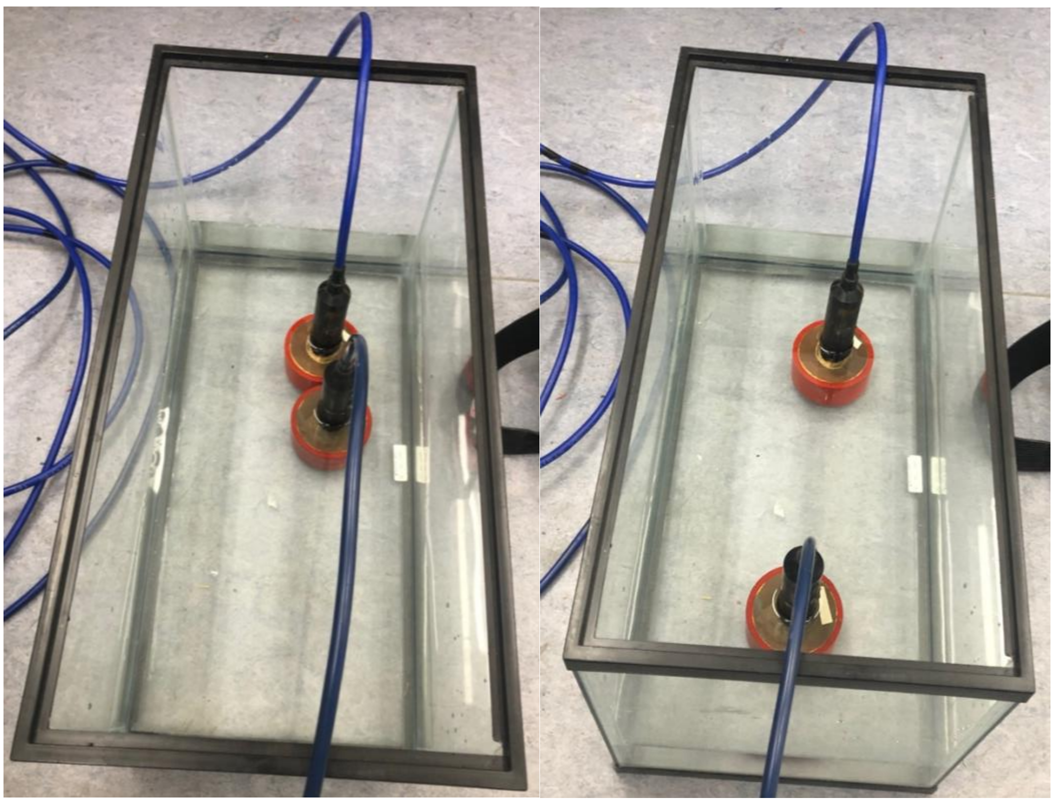

Figure 18: two hydrophones, placed in a small glass fish tank for initial testing

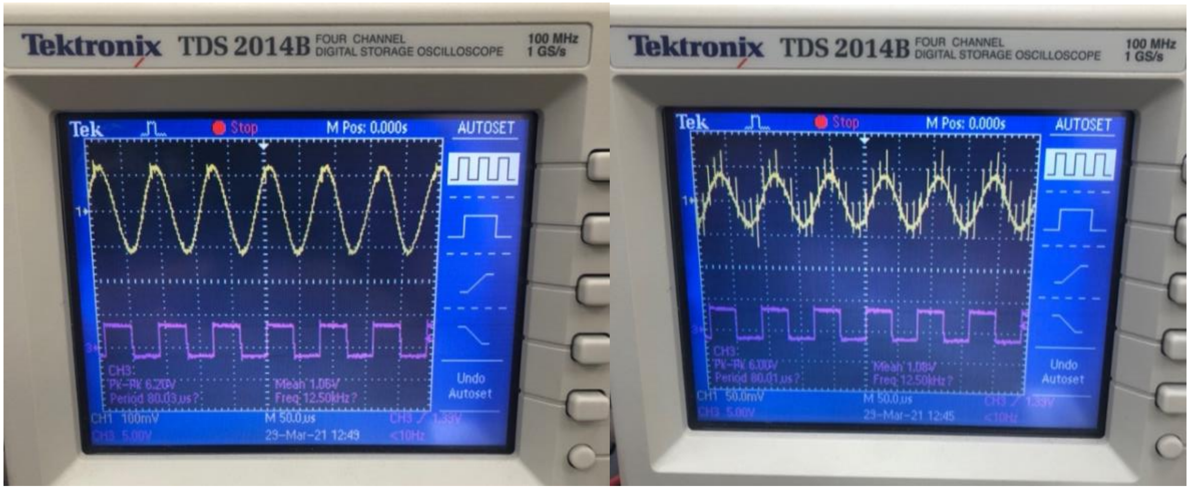

Figure 19: Waveform received while hydrophones were physically touching in tank (left) versus a small separation (right)

The pre-amp circuit was a simple design using a non-inverting topology and JFET operational amplifier chip and an adjustable feedback resistor implemented with a potentiometer. The pre-amp was initially tested using a function generator as its input. Using this off-the-shelf source isolated the testing to a single new component (the pre-amp). Both pre-amps showed good frequency response and minimal phase-shift as shown in figure 20 below.

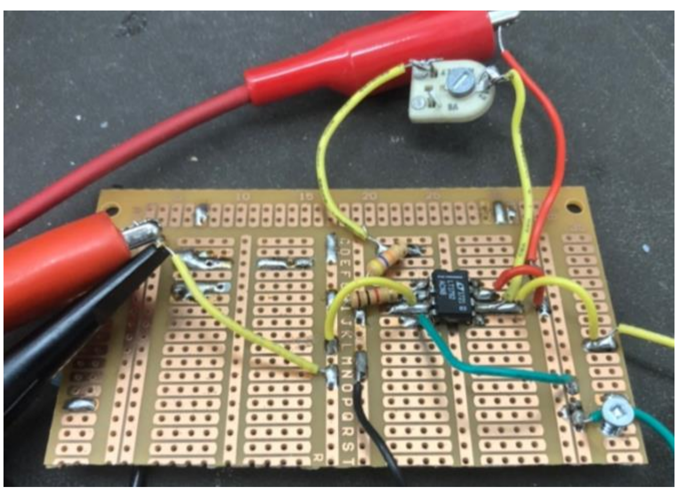

Figure 20: pre-amp circuits with tuneable gain via feedback potentiometer

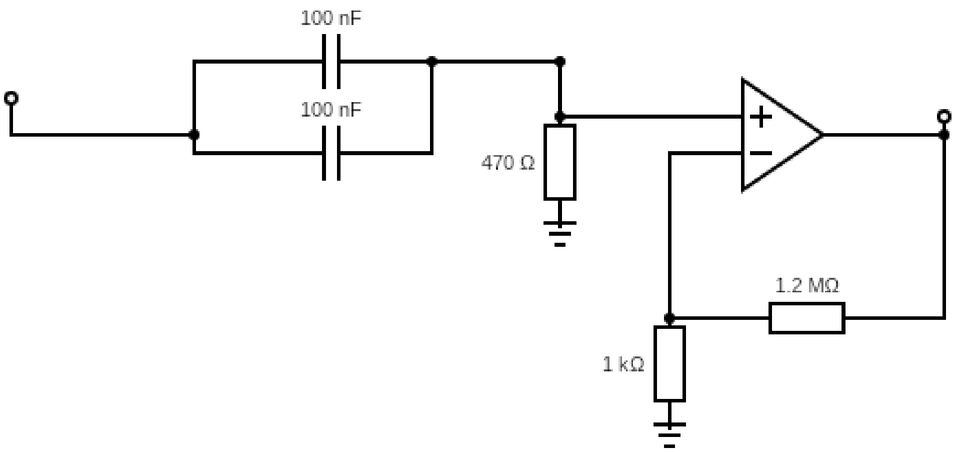


Figure 21: Schematic of pre-amplifier receiver circuit

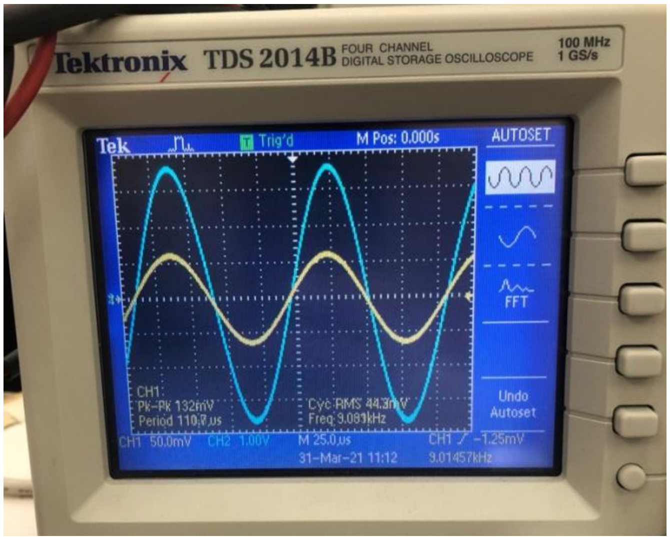


Figure 22: Testing the pre-amp with a function generator input

Once tested in the tow tank, the pre-amp performance was immediately evident. In Figure 23 below, the yellow signal with no visible signal in the 12.5 kHz band is the input to the pre-amp while the blue signal is its output signal. The pre-amp input was connected to a passive high-pass filter at the input comprising of two parallel 0.01 microfarad capacitors (at the input) and a 470 Ω resistor (tied to ground), with the centre-point connecting to the amplifier input. This effectively eliminated the 60 Hz signal present in the water by creating a high impedance (large

% voltage drop) at 60 Hz but a low impedance (small voltage drop) at 12.5 kHz., preserving the high-frequency voltage for amplification.

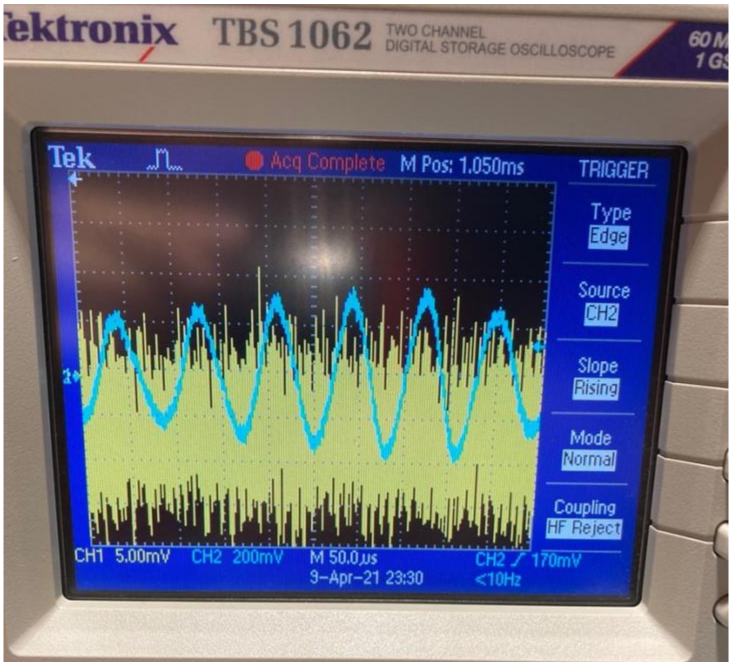

Figure 23: pre-amp performance in the tow bank. Yellow is input signal and blue is output signal.

Before installing the trigger-connection coaxial cable, the full system was tested on the same bench, with the hydrophones in open air. This experiment ensured that the system's interconnection was functioning before the 120 feet of coaxial cable was strung along and secured to the edge of the tank. The setup connected to the same trigger signal (low side of the inverter signal)

With all the components tested individually, it was time to test the full system in the experiment environment. In Figure 24 below, both the signal observed near the transmitter and the received signal are shown on the same plot. This signal plot was considered for validity before continuing with the experiment trials. Knowing the full displacement was 45.8 meters and approximating the speed of sound in water to be 1500 m/s, seeing the received signal arrive at just over 0.03 seconds lined up with the expected outcome (0.03 x 1500 = 45) as well as the observer signal being picked up at approximately 0.7 ms (0.007 seconds x 1500) or approximately 10 meters into the interval. These high-level estimations show the received signals line up with the expected time estimates.

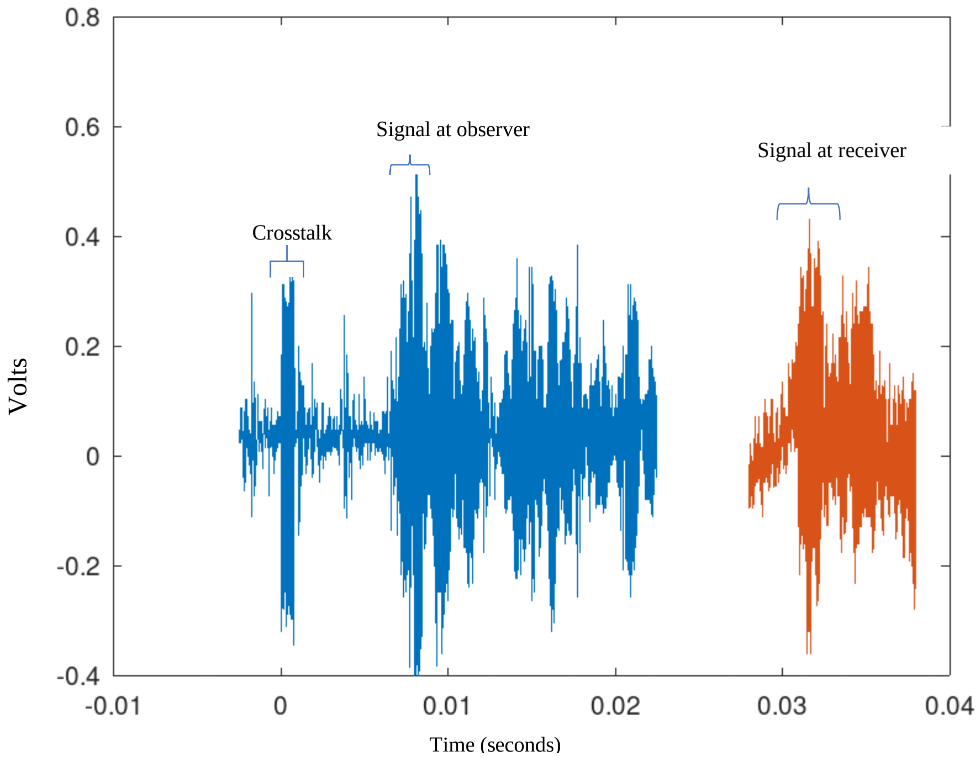


Figure 24: The hydrophone signal recorded at the observing hydrophone (blue) and the receiver-side hydrophone (orange)

## 4.3 Conclusion

In summary, this section discusses system design consideration and the process of testing the system components. Where possible, this system uses cost-effective, off the shelf components to reduce unnecessary complexity and improved reliability. The system components were tested modularly to assess their operation before being integrated and validated in a complete system test.

# CHAPTER 5: Data Analysis

## 5.1 Analysis

In order to determine the travel-time of the acoustic signal, a cross-correlation analysis was performed.  A cross-correlation is a measure of the similarity of two signals. By finding the cross-correlation between the transmitted waveform and the waveform received at the receiver, the original waveform can be detected in the received waveform, thus providing a measurement of time elapsed between the transmission and reception of the acoustic signal.

GNU Octave, a powerful open-sourced numeric computing platform was used to perform the analysis operations. Octave has a package for signal analysis (‘signal’) that provided a cross-correlation function, xcorr2, to compare the waveforms from the transmitting side, observing hydrophone and the receiving side.

Octave supports use of a for loop which greatly sped up the analysis. The analysis was conducted in the following steps:

1) Resample the observer hydrophone’s signal to match the 4-microsecond rate used on the receiver-side oscilloscope

2) Compute the cross-correlation of a sub-section of the observer hydrophone’s data set i.e. 200 - 1000 samples

3) Determine the maximum point of the cross-correlation results and capture the associated index number

4) Repeat for various ranges, ranging from the length of 10 transmitted pulses up to many times that duration (these were manually edits and the script was then ran again)

Below is the octave script used to obtain the cross-correlation peaks:

```
pkg load signal;

for i = 1: length(tx_list)
        tx_exp1_1_csv = csvread(tx_list(i).name);
        rx_exp1_1_csv = csvread(rx_list(i).name);
        tx_resample = resample(tx_exp1_1_csv,10,4);
        xcor = xcorr2(tx_resample(1700:1900,2),rx_exp1_1_csv(:,2));
        [x,ix] = max(xcor);
        disp(ix);
end
```

Once all these computations were completed, the data was exported to CSV file for further analysis. Within the spreadsheeted, standard deviation was calculated for each permutation of sample range, using libre office's built-in STDEV() function. From these calculated parameters, it was clear to see that as the sample window got closer and closer to just containing the initial 10 pulses, the standard deviation decreased rapidly while the variance from a theoretical target value became smaller as well.

| Samples Used | Standard Deviation of 45 Trials (# of samples) |
|---|---|
| Old Method | 494.90 |
| 200 samples | 124.86 |
| 400 samples | 300.83 |
| 600 samples | 309.14 |
| 800 samples | 307.46 |
| 1000 samples | 301.32 |

Figure 25: table showing standard deviation versus cross-correlation inputs

## 5.2 Resampling Data

During the setup of the experiment, while adjusting the oscilloscopes, the horizontal scale was unknowingly changed on the settings for the observing hydrophone. This variance was not noticed while the experiment was being conducted and was only noticed during initial analysis. To make this data set useful, it was necessary to resample the data in order to have a consistent sampling rate between both oscilloscopes, in order to perform a proper cross-correlation. Thankfully, octave has a function to resample data. Using the resample() function, the data was able to be converted to 4 microsecond samples versus the original 10 microsecond rate. With the datasets now configured properly, analysis could be undertaken. Figure 26 below shows some of the data that was resampled with the original signal in orange and the resampled signal in blue. There was minimal impact on the data quality due to this resampling.

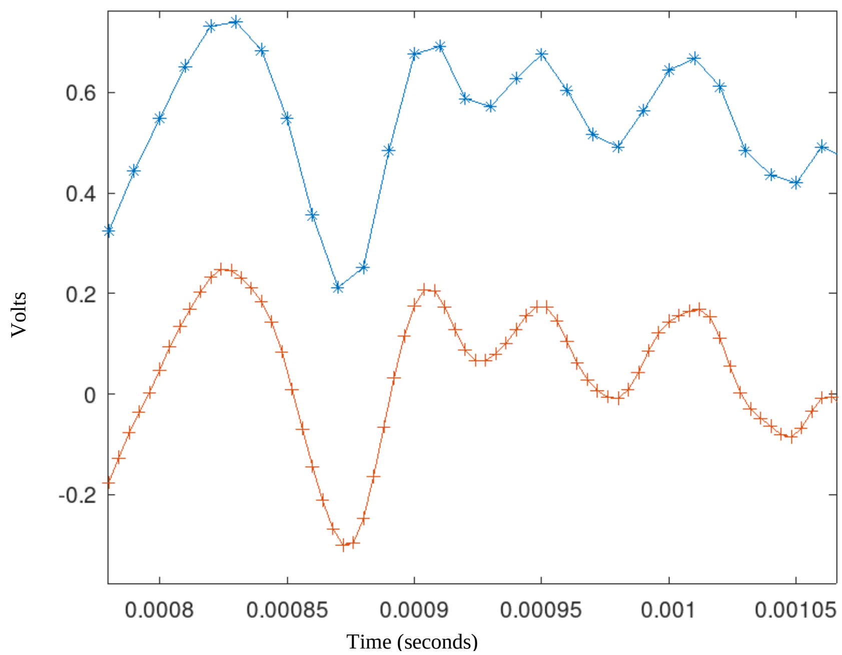


Figure 26: the original dataset (in blue, offset) above the resampled, version (orange).

## 5.3 Results

The results from the cross-correlation were consistent over each of the 45 trials conducted. The original technique, used in Mr. Smith's thesis, would detect a local peak near the expected result but there was also a global maximum value that was much earlier in the time-frame and resulted in the incorrect value being selected using the max() function in Octave. It is believed that by not accounting for the environment's impact on shaping the transmitted waveform and instead using an ideal, assumed output waveform for this analysis technique fails to differentiate between the transmitted waveform and the various multipath arrivals (interference), which has the same frequency and other general characteristics.

The new technique measures the waveform in the aqueous environment with various non-ideal characteristics imposed on it by the tank environment and uses this data to perform a more accurate cross-correlation. It can be observed in Figure 27 and Figure 28 below that the same characteristic wave that appears to be a sine wave superimposed onto a triangle wave, around the 1700 sample mark. This waveform looks like what one would expect from an ideal cross-correlation of two identical sinusoidal waveforms; the correlation grows as the overlap becomes a greater percentage of the signal's duration while the sinusoidal nature shows that as opposing peaks and troughs overlap, that they are then quite opposite and inversely correlated and generate a negative result.

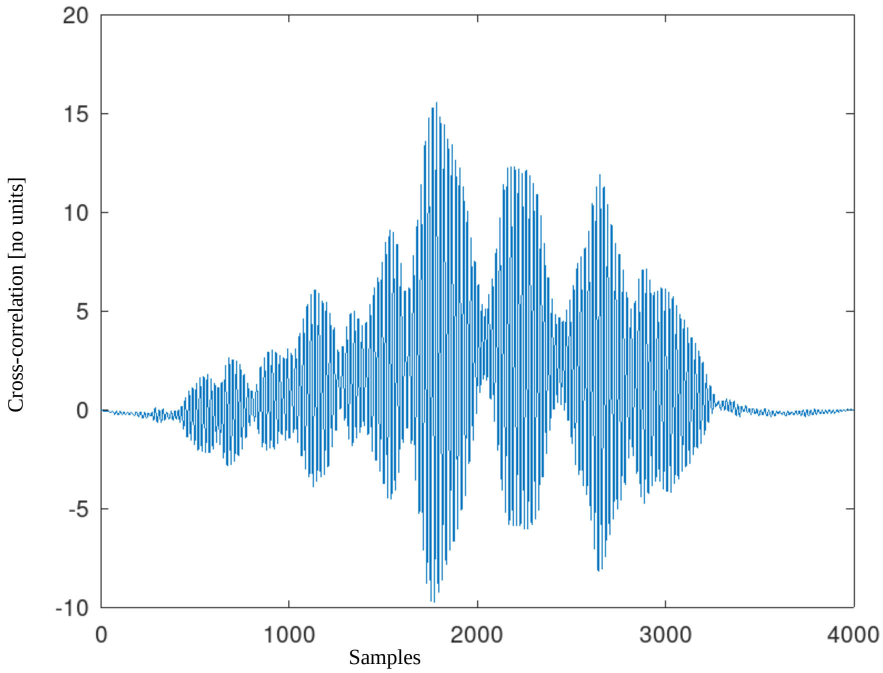


Figure 27: cross-correlation output from new technique (x-axis is in samples)

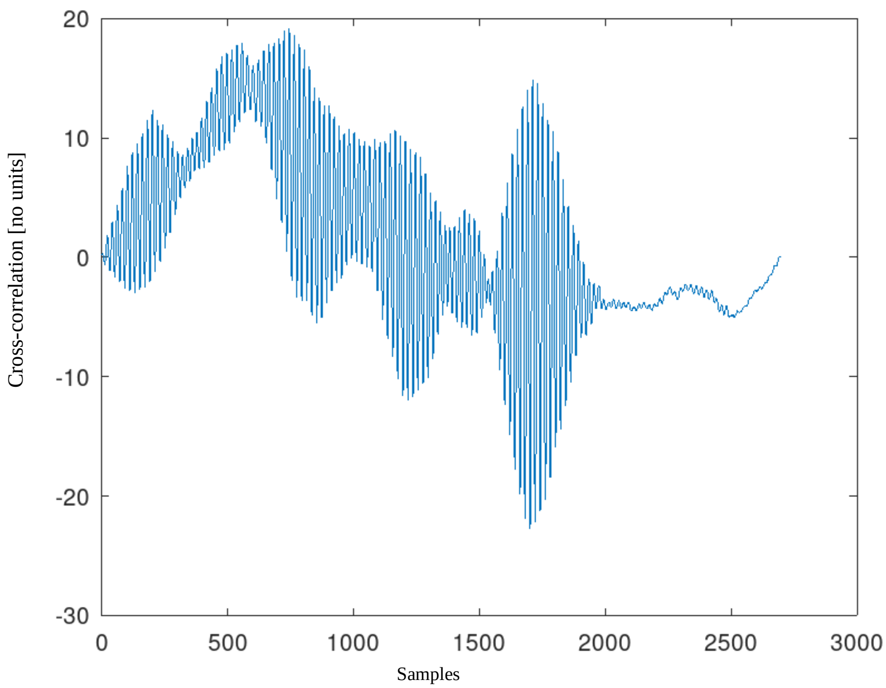


Figure 28: cross-correlation output from the old technique (x-axis is in samples)

The results from Tim Smith's thesis [10], the results required manual review and occasional correction when larger discrepancies occurred. The results from this new technique have not been manually altered and only one of the trials yielded a result that deviated significantly from the average value (see Figure 29 above, trial 12). This single deviation represented just over 2% of the trials and can be considered an outlier in the dataset.

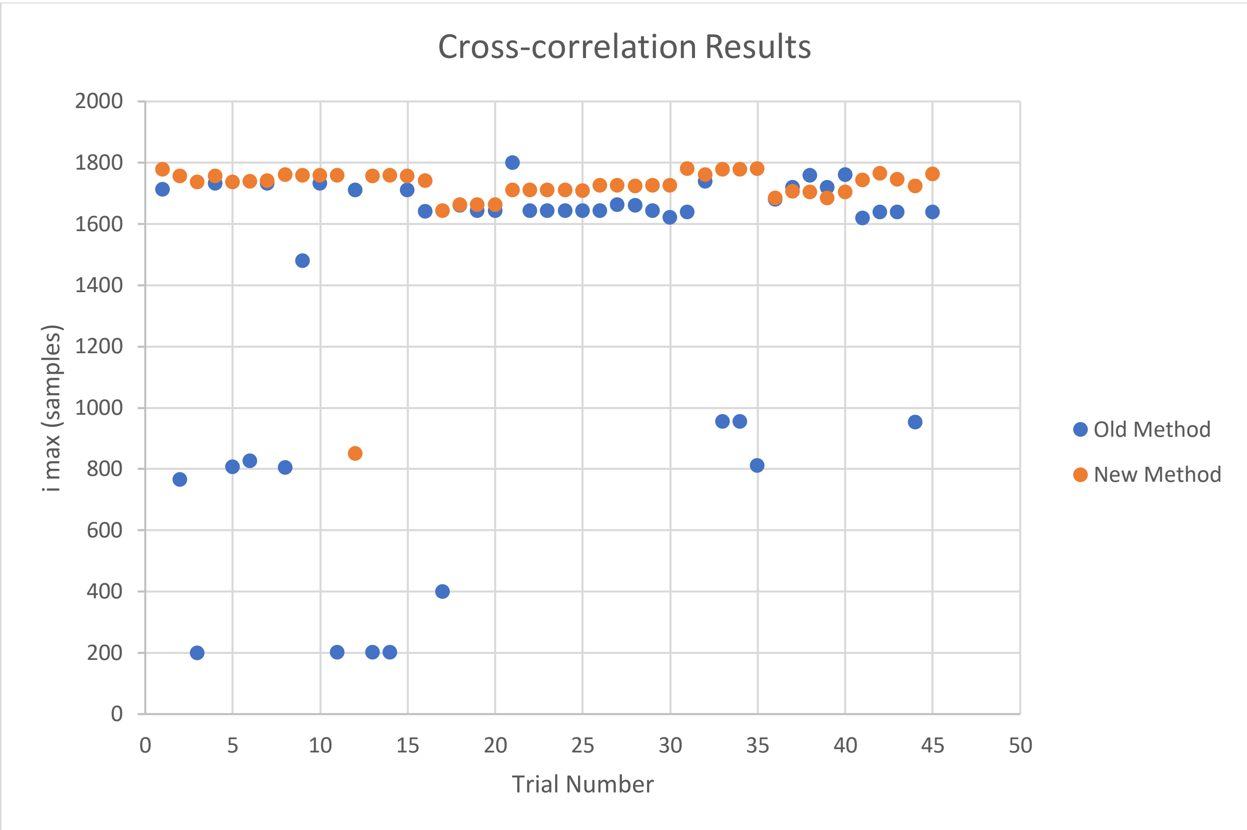


Figure 29: cross-correlation results for all trials using a 200-sample window for the input signal (orange) and the original method approach shown in blue

## 5.4 Conclusion

In summary, this section discusses the data analysis performed to assess the relative performance of the two approaches employed. The new approach was shown to be more consistent in its determination, as shown by a reduced standard deviation as well as its accuracy. As well, importantly, these results did not require any manual interpretation and were entirely based on scripted analysis.

# Chapter 6: Conclusion

## 6.1 Summary

Previously, an acoustic tomography system, developed and tested by Tim Smith [10] attempted to use a bi-directional acoustic time-of-flight approach to measure ocean currents. This prior approach utilized an ideal signal, with timing measured at the microcontroller and a complex, MODBUS-based time synchronization method which led to results that required manual revisions.

The new approach detailed in this document utilized real-world data captured after electric-to-piezo excitation of the hydrophone was performed and this revised approach which did not require manual intervention. Only one of the forty-five trials has a result that was a large variation from the expected outcome compared to a frequent amount in the previous work [10]. This new approach was also validated experimentally, despite the access restrictions on facilities imposed by covid-19. This work has been presented at the 2021 IEEE NECEC conference in St. John’s, NL [16].

The experiment detailed in this thesis set out to make a proof-of-concept for a novel technique to improve the accuracy and precision of time-of-flight based acoustic tomography measurements. The results from this preliminary study are promising, they show a greatly improved result in the towing tank test environment, as demonstrated by the reduced standard deviation in the experimental trials.

## 6.2 Future Work

The contributions of this thesis lay the groundwork for scaled-up oceanographic acoustic tomography experiments in the future. This proof-of-concept can be expanded by adding additional techniques to improve the practical use case for shorter range OAT such as digital modulation schemes (instead of a fixed PWM driving signal) as well as using wireless communications for time synchronization, as opposed to the fixed connection used in the proof of concept. Future work in this area could also perform trials in a field setting with the full bi-directional transmission sequence conducted and compare its results with an established method for measuring current speeds, such as an ADCP.

## 6.3 Conclusion

This thesis detailed a novel approach to improve time-of-flight acoustic tomography systems. The initial experiments with this system were promising and showed improved accuracy, reduced standard deviation, and removed the need to manually interpret the results of the signal analysis. However, this is just the beginning of further testing required to extensively evaluate this approach. It is recommended that these initial trials be supplemented by field testing and improvements to system components, such as utilizing for robust modulation schemes in the hydrophone diver.

# Bibliography

[1] T. Georges and W. Woodward, *MEASURING OCEAN CURRENTS WITH HF RADAR,* NOAA.

[2] G. BOLD, C. CHIU, B. COLOSI, B. CORNUELLE, B. DUSHAW, M. DZIECIUCH, A. FORBES, F. GAILLARD, L. GOULD, B. HOWE, M. LAWRENCE, J. LYNCH, D. MENEMENLIS, J. MERCER, P. MIKHALEVSKY, W. MUNK, I. NAKANO, F. SCHOTT, U. SEND, R. SPINDEL, T. TERRE and P. WORCESTER, "OceanObs'09," 17 September 1999. [Online]. Available: http://www.oceanobs09.net/work/oo99/docs/Wunsch.pdf. [Accessed 20 09 2021].

[3] N. Hogg and D.E. Frye, "Performance of a new generation of acoustic current meters," *Journal of Physical Oceanography,* vol. 37, no. 2, pp. 148-161, 2007.

[4] D. Rosenfield, J. Caruthers, D. Nechaev, G. Ioup, J. Ioup, N. Sidorovskaia and M. Yaremchuk, "Using Acoustic Tomography to Monitor Deep Ocean Currents in the Eastern Gulf of Mexico," *OCEANS 2009,* pp. 1-3, 2009.

[5] A. Joesph, Measuring Ocean Currents Tools, Technologies and Data, Waltam, MA: Elsevier, 2014.

[6] E. L. Mills, "Studying The Oceans and the Oceans," in *The Fluid Envelope of our Planet*, Toronto, University of Toronto Press, 2009, pp. 258-286.

[7] V. Klemas, "Remote Sensing of Coastal and Ocean Currents: An Overview," *Journal of Coastal Research* , vol. 28, no. 3, pp. 576-586, 2012.

[8] W. E. Baxley, *OCEAN CURRENT MEASUREMENTS: CHALLENGES AND OPPORTUNITES IN THE FLORIDA CURRENT,* Fort Lauderdale: Nova Southeast University, 2013.

[9] T. Gytre, "Acoustic Travel Time Current Meters," in *Air-Sea Interaction*, Boston, Springer, 1980, pp. 155-170.

[10] T. Smith, *Measuring Marine Currents Using Underwater Acoustics*, St. John's, Newfoundland: Memorial University, 2020.

[11] P. Holstein, A. Raabe, R. Muller, M. Barth, D. Mackenzie and E. Starke, "Acoustic tomogrpahy on the basis of time-travel measurement," *Measurement Science and Technology,* pp. 1420-1428, 2004.

[12] F. Dobson, L. Hasse and R. Davis, "Survey of Techniques for Measuring Currents near the Ocean Surface," in *Air-Sea Interaction*, Boston, Springer, 1980, pp. 228-232.

[13] P. F. Worchester, W. H. Munk and R. C. Spindel, "Acoustic Remote Sensing of OCean Gyres," *Acoustics Today,* pp. 11-17, 2005.

[14] L. Angrisani, A. Baccigalupi and R. Schiano Lo Moriello, "Ultrasonic Time-of-Flight Estimation Through Unscented Kalman Filter," *IEEE Transactions on Instrumentation and Measurement,* vol. 55, no. 4, pp. 1077-1084, 2006.

[15] C. Capps, "Near field or far field," *edn magazine,* pp. 95-102, 16 August 2001.

[16] J. Blackwood, "Novel Technique to Improve the Measurement of Acoustic Tomography," in *IEEE NECEC*, St. John's, 2021.